Dalton Transactions

Accepted Manuscript

This article can be cited before page numbers have been issued, to do this please use: Y. Wang, R. Song, K. Guo, Q. Meng, R. Zhang, X. Kong and Z. Zhang, *Dalton Trans.*, 2016, DOI: 10.1039/C6DT02229D.

ROYAL SOCIETY OF CHEMISTRY

www.rsc.org/dalton

View Article Online
DOI: 10.1039/C6DT02229D

Journal Name

ARTICLE

Gadolinium(III) Complex based Dual-Modal Probe for MRI and Fluorescence Sensing of Fluoride ion in Aqueous Medium and *in vivo*

Received 00th January 20xx,

Accepted 00th January 20xx

DOI: 10.1039/x0xx00000x

www.rsc.org/

Yue Wang,[a] Renfeng Song,[b] Ke Guo,[b] Qingtao Meng,[a]* Run Zhang,[a,c] Xiangfeng Kong[a] and Zhiqiang Zhang[a]*

A novel Gd(III) complex, Gd(TTA)$_3$-**DPPZ** was designed and assembled as a dual-modal probe for the simultaneous fluorescence and magnetic resonance imaging (MRI) detection of fluoride ion in aqueous media and *in vivo*. In this system, Gd(III) center is not only serving as a MRI signal output unit, but also proving a binding site for fluoride ion. When apropos equivalents of fluoride ions were added into the solution of Gd(TTA)$_3$-**DPPZ**, the replacement of the coordination water led to decrease of the longitudinal relaxivity (r_1) as well as the distinct spectroscopic changes, by which MRI/fluorescence dual-modal fluoride ion sensing was achieved. In the present of fluoride ions, 2-fold fluorescence emission enhancement of Gd(TTA)$_3$-**DPPZ** , and a notable decrease of the UV–vis absorption spectrum were observed. The fluorescent detection limit for fluoride ion was established at 70 nM. Gd(TTA)$_3$-**DPPZ** also exhibits about 75% decrease of the longitudinal relaxivity (r_1) upon addition of fluoride ions in aqueous medium. The appropriate blood circulation time of Gd(TTA)$_3$-**DPPZ** allows potential application in MRI *in vivo*. The results demonstrated that Gd(TTA)$_3$-**DPPZ** could serve as a potential MRI/fluorescence bimodal imaging agent for the specific and high-sensitive sensing of fluoride ions *in vivo*.

Introduction

To elucidate the important roles of bioactive ions and molecules to health and disease, biologists and biochemists are initiating a broad-based program to develop new chemical approaches to study aspects of their uptake, trafficking, export, and functions in living systems.[1] At present, fluorescence imaging, due to its high sensitivity, operational simplicity, specificity, and biocompatibility, is recognised as one of the most powerful tools to visualize these ions and molecules in complicated biological processes.[2,3] Although fluorescence imaging probes have been widely exploited in biotechnology and biomedical research fields, non-invasive *in vivo* molecular imaging applications were limited due to the shallow penetration depth of incidence light.[4,5] In contrast to optical microscopy imaging technology, magnetic resonance imaging (MRI) has recently been explored as a non-invasive imaging technique that allows images of intact, opaque organisms in three dimensions without photobleaching or light scattering.[6-8] Unfortunately, as each detection method has its own considerations, MRI technique has just been able to resolve objects larger than a few micrometers in size, thus exhibiting much lower resolution than optical analysis.[9] Therefore, integration of fluorescence and MRI technique in one setting is appealing due to the complementary nature of high penetration depth of MRI and high resolution of fluorescence analysis.[10] Currently, Gd(III) complexes based MRI/fluorescence dual-modal probes have been widely used for sensing and imaging of metal ions and biological molecules in both aqueous medium and biological systems.[11-14] However, to the best of our knowledge, few of Gd(III) complexes based MRI/fluorescence probes have been developed specific for the detection of anions.

Anions play fundamental roles in biological, security and environmental science.[15-17] Among various important anions, fluoride ion in biological system, as the smallest and most electronegative anion, has been received increasing attention in recently years. It has been well documented that intake of acute amount of fluoride anions is beneficial to the treatment of osteoporosis and dental health.[18-20] However, excessive intake of fluoride ion may induce various diseases, such as gastrointestinal dysfunction, dental fluorosis, bone fluorosis, and so on.[21,22] Therefore, rapid, sensitive, specific, and accurate detection of fluoride ion *in vivo in-situ* is of great importance for investigating its functions in environmental and biological samples. In particular, to meet the requirements in

[a] *School of Chemical Engineering, University of Science and Technology Liaoning, 185 QianshanZhong Road, Anshan, 114051, P. R. China. Email: qtmeng@ustl.edu.cn; zhangzhiqiang@ustl.edu.cn. Tel: Tel: +86-421-5928009*
[b] *Ansteel Mining Engineering Corporation, 27 Lvhua Street, Anshan,114002,P. R. China*
[c] *Australian Institute for Bioengineering and Nanotechnology, The University of Queensland, Brisbane, 4072, Australia*
† *Footnotes relating to the title and/or authors should appear here.*
Electronic Supplementary Information (ESI) available: [details of any supplementary information available should be included here]. See DOI: 10.1039/x0xx00000x

View Article Online
DOI: 10.1039/C6DT02229D

the practical applications in biological samples, receptors that could be used for specific detection of fluoride ions in aqueous solution are highly desirable. But detection of fluoride in water remains a challenge due to the high free energies of hydration of this anion.[23] Among numerous anion receptors, organic lanthanide complexes have been recognised to be the excellent candidates to develop of molecule imaging probes for the detection of anions because of their unique photophysical and photochemical properties.[24-26] By virtue of high affinity of the targeted anions and hard Lewis acid nature of lanthanide ions, the specific interaction of anions with lanthanide(III) center led to the liberation of the coordinated water molecule. Consequently, specific response in signals, such as colour,[27] MRI and fluorescence could be achieved as the basic mechanism for anions sensing.[28,29]

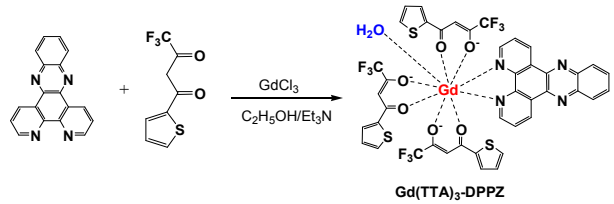

Scheme 1 Proposed structures of Gd(TTA)$_3$-**DPPZ**

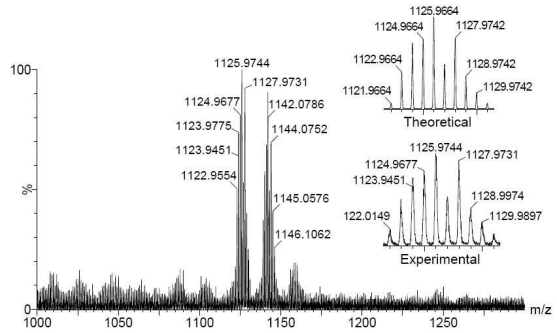

Fig. 1 ESI-MS spectrum of Gd(TTA)$_3$-**DPPZ**.

Due to the high magnetic moment (μ^2 = 63 μB^2), and a symmetric electronic ground state, $^8S_7/_2$ of Gd(III) ions, Gd(III) complexes have long been clinically used as the MRI contrast agent.[30] As the Solomon-Bloembergen-Morgan theory described, the relaxivity of Gd(III) complexes are governed by a variety of factors including the number of bound water molecules (q), the rotational tumbling times (τ_R) and the mean residence lifetime of Gd(III)-bound water molecules (τ_M).[31] Typically, the MRI signal of Gd(III) complexes are expected to be finely tuned by changing in q upon treatment of targeted ions or molecules in aqueous solution.[32,33] Inspired by this strategy,[34-36] in this work, a Gd(III) complex, Gd(TTA)$_3$-**DPPZ**, was developed for the detection of fluoride ions in both aqueous medium and mice. Gd(TTA)$_3$-**DPPZ** was designed by employing a β-diketonate derivative, thenoyltrifluoroacetonate (TTA) as the ligand due to its ideal complexation with lanthanide ions.[37] The Gd(III) centre also provides high electrostatic interaction to bind negatively charged fluoride ion. Gd(TTA)$_3$-**DPPZ** has a mononuclear nine-coordinate structure in which Gd(III) is surrounded by two nitrogen atoms from phenanthroline derivative, six oxygen atoms of tris(2-thenoyltrifluoroacetonate) and one coordinated water molecule.[38] In the presence of fluoride ions, the replacement of water molecules led to the decreasing the longitudinal relaxivity (r_1) as well as the distinct spectroscopic changes,[39] realizing MRI/fluorescent dual modal sensing of fluoride ion in aqueous and biological samples.

Results and Discussion

Synthesis and characterization of Gd(TTA)$_3$-DPPZ

The designed neutral and unsaturated complex, Gd(TTA)$_3$-**DPPZ**, was synthesized by a one-step complexation of TTA and 4,5,9,14-tetraaza-benzotriphenylene (**DPPZ**) with Gd(III) ions in ethanol (Scheme 1). The structure and purity of Gd(TTA)$_3$-**DPPZ** was well characterized by ESI-MS, HPLC, and elemental analysis. As shown in Fig. 1, ESI-MS spectrum of Gd(TTA)$_3$-**DPPZ** in solution exhibited two intense peaks at m/z = 1125.9744 and 1142.0786, which can be assigned to the species of [Gd(TTA)$_3$-**DPPZ** + Na]$^+$ and [Gd(TTA)$_3$-**DPPZ** + K]$^+$, respectively (Fig. 1 and Fig. S2, ESI†). HPLC analysis exhibited that the retention time of Gd(TTA)$_3$-**DPPZ** was at 2.16 min by using methanol as the eluent. The purity of Gd(TTA)$_3$-**DPPZ** was determined to be 99.3%.

Gd(TTA)$_3$-**DPPZ** showed pH independent in the range of 4.0–10.0 (Fig. S3, ESI†), indicating that the complex Gd(TTA)$_3$-**DPPZ** is suitable for application under physiological conditions. Gd(TTA)$_3$-**DPPZ** shows desired stability in aqueous medium (THF: H_2O = 5:5) at pH = 7.4. As shown in Fig. S4, there were no obvious changes of fluorescent intensity within 30 h, indicating that Gd(TTA)$_3$-**DPPZ** is stable under the test condition.

Spectroscopic studies of Gd(TTA)$_3$-DPPZ in the presence of anions

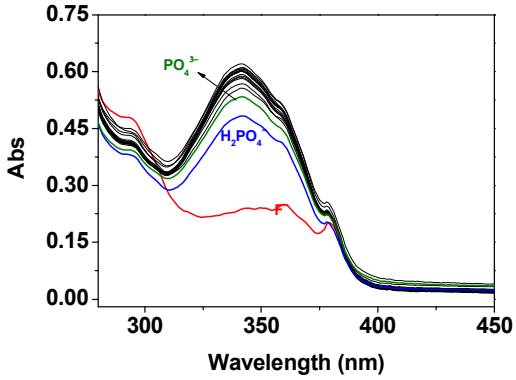

Fig. 2 UV-vis absorption spectra of Gd(TTA)$_3$-**DPPZ** (10 μM) in H_2O (THF: H_2O = 5:5, pH = 7.4) upon addition of various anions: 0.7 mM of Br^-, NO_3^-, OH^-, I^-, HSO_4^-, AcO^-, $H_2PO_4^-$, F^-; and 100 mM Cl^-; 1 mM PO_4^{3-}.

View Article Online
DOI: 10.1039/C6DT02229D

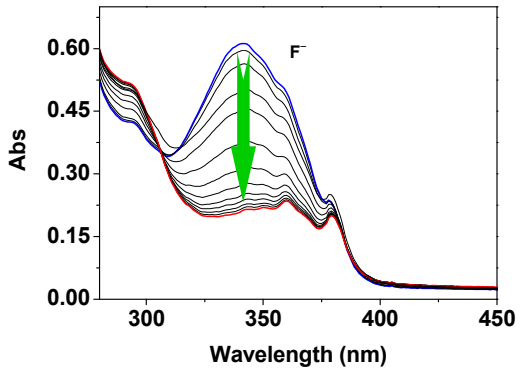

Fig. 3 UV-vis absorption spectra of Gd(TTA)$_3$-**DPPZ** (10 μM) in the presence of increasing amount of fluoride ions (0–0.7 mM) in H_2O (THF: H_2O = 5:5, pH = 7.4).

By virtue of the high affinity of the fluoride with lanthanide(III) ions, Gd(TTA)$_3$-**DPPZ** was expected to act as a potential indirect probe for fluoride ion sensing *via* displacement of coordinated water molecule. Thus, the response of fluoride ion by Gd(TTA)$_3$-**DPPZ** complex was firstly investigated by spectrophotometric titration in aqueous medium (THF: H_2O = 5:5, pH = 7.4). As showed in Fig. 2, Gd(TTA)$_3$-**DPPZ** displayed a major absorption band with a maximum absorption peak at about 340 nm in aqueous medium, which can be attributed to over-lap of the thenoyltrifluoroacetone (TTA) ligand and phenanthroline derivative (**DPPZ)** (Fig. S5, ESI†).[40] As shown in Fig. 2, upon the addition of diverse anions, including 0.7 mM of AcO^-, Br^-, NO_3^-, I^-, HSO_4^-, OH^-, even 100 mM Cl^- and 1 mM PO_4^{3-}, no obvious changes in absorption spectra of Gd(TTA)$_3$-**DPPZ** were observed. The absorption spectrum was slightly changed upon the titration of 0.7 mM $H_2PO_4^-$. In contrast, a remarkable decrease in the absorbance peak at 340 nm with a 20 nm bathochromic shift of absorbance band were observed when fluoride ions (0-0.7 mM) was added (Fig. 3). The results demonstrated that Gd(TTA)$_3$-**DPPZ** can be employed as a specific probe for fluoride ion sensing in aqueous solution.

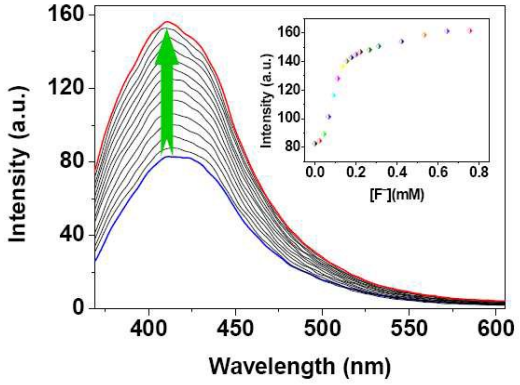

Fig. 4 Fluorescence spectra of Gd(TTA)$_3$-**DPPZ** (10 μM) in the presence of different amounts of fluoride ions (0–0.7 mM) in H_2O (THF: H_2O = 5:5, pH = 7.4). Insert: Normalized fluorescence intensities of Gd(TTA)$_3$-**DPPZ** (10 μM) at 420 nm as a function of fluoride ion concentration. Excitation was performed at 340 nm.

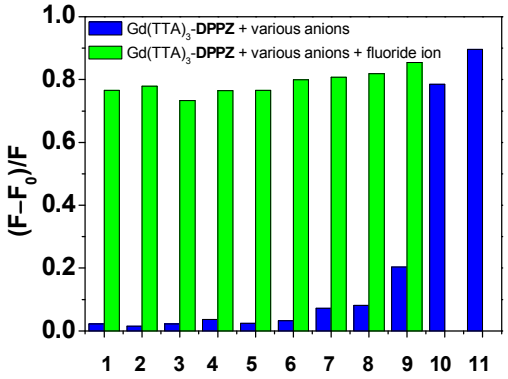

Fig. 5 Changes in fluorescence intensity of Gd(TTA)$_3$-**DPPZ** (10 μM) toward fluoride ion in the presence of various competing anions in H_2O (THF: H_2O = 5:5, pH = 7.4): (1) Br^- (0.7 mM), (2) Cl^- (100 mM), (3) NO_3^- (0.7 mM), (4) OH^- (0.7 mM), (5) I^- (0.7 mM), (6) HSO_4^- (0.7 mM), (7) AcO^- (0.7 mM), (8) PO_4^{3-} (1 mM), (9) $H_2PO_4^-$ (0.7 mM), (10) F^- (0.7 mM), (11) Anions mixed. The intensities were recorded at 420 nm, excitation at 340 nm.

Fluorescent titration analysis was then conducted to demonstrate the capability of Gd(TTA)$_3$-**DPPZ** ensemble as the probe for fluoride ion sensing in aqueous medium (THF: H_2O = 5:5, pH = 7.4). As shown in Fig. 4, the fluorescence emission of Gd(TTA)$_3$-**DPPZ** was gradually switched "ON". A ca. 2-fold enhancement of fluorescence intensity was observed when the addition of 0.7 mM fluoride ions. The fluorescence enhancement could be attributed to the displacement of coordination water molecules by fluoride ions in close proximity to the Gd(III).[41] In addition, the increase in fluorescence intensity was found partly contributed by the interaction of fluoride ion and TTA ligand (Fig. S6, ESI†). No changes in absorption and fluorescence spectra of **DPPZ** ligand was noticed in the presence of fluoride ions. The enhancement of fluorescence intensities showed a good linearity with the concentrations of fluoride ions in the range of 0–50 μM and the detection limit was estimated to be 70 nM based on a 3σ/slope by reported method (Fig. S7, ESI†).[42,43] In addition, the selectivity of Gd(TTA)$_3$-**DPPZ** towards fluoride ion was also evaluated by fluorescence analysis. As shown in Fig. 5, no significant fluorescence enhancements were observed when Gd(TTA)$_3$-**DPPZ** was treated with AcO^-, Br^-, NO_3^-, I^-, HSO_4^-, OH^-, and tremendously excessive amounts of Cl^- (100 mM) and PO_4^{3-} (1 mM). The addition of $H_2PO_4^-$ into Gd(TTA)$_3$-**DPPZ** solution led to slight increase in fluorescent intensity compared to that of fluoride ions (4.5 times smaller). The excellent selectivity could be attributed to the higher affinity of Gd(TTA)$_3$-**DPPZ** system to fluoride ion over other typically anions. In addition, to evaluate the utility of Gd(TTA)$_3$-**DPPZ** for the selective detection of fluoride ion in a complicated environment, Gd(TTA)$_3$-**DPPZ** solution was treated with fluoride ion in the presence of different competitive anion species. All potentially competitive anions exerted no or little influence on the fluorescence detection of fluoride ion, suggesting that Gd(TTA)$_3$-**DPPZ** is a fluoride-specific fluorescence probe even in complicated samples.

View Article Online
DOI: 10.1039/C6DT02229D

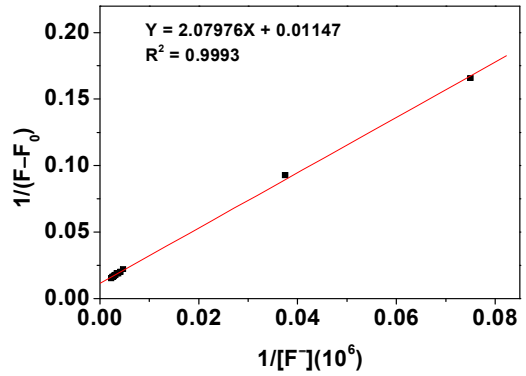

Fig. 6 Benesi-Hildebrand plot of Gd(TTA)$_3$-**DPPZ** (2 μM) in H_2O (THF: H_2O = 5:5, pH = 7.4) based on 1:1 binding stoichiometry with fluoride ions. The intensities were recorded at 420 nm, excitation at 340 nm.

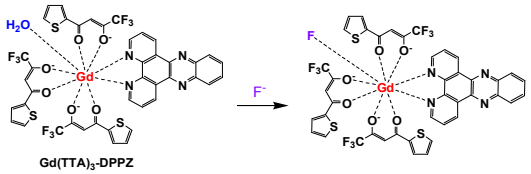

Scheme 2 The proposed mechanism for fluoride ion sensing by Gd(TTA)$_3$-**DPPZ**

To verify the replacement of waters with fluoride ions, the binding mode of Gd(TTA)$_3$-**DPPZ** toward fluoride ion was determined by using the Benesi–Hildebrand equation.[44] As shown in Fig. 6, the plotting of 1/(F − F_0) versus 1/[fluoride] showed a good linear relationship (R^2 = 0.9993), which indicates a stable 1:1 stoichiometry complexation species, and the association constant K_a was calculated to be $7.35 \times 10^3\ M^{-1}$. The results further indicated that the coordination waters replacement mechanism is responsible for the spectroscopic responses towards fluoride ions.

MRI Responses toward fluoride

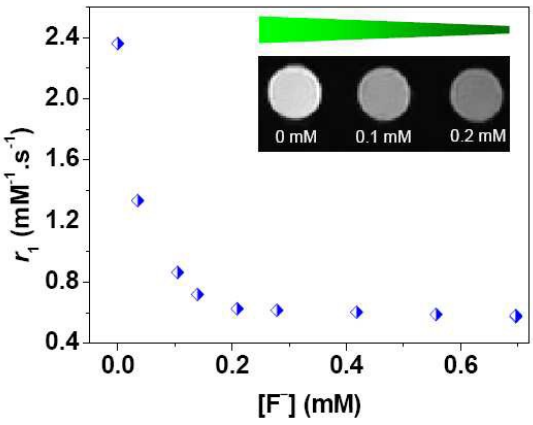

Fig. 7 Changes in the longitudinal relaxivity (r_1) of Gd(TTA)$_3$-**DPPZ** (0.2 mM) as a function of fluoride ions concentration (0-0.7 mM) in H_2O (THF: H_2O = 5:5, pH = 7.4). Insert: T_1-weighted MR images of Gd(TTA)$_3$-**DPPZ** recorded *versus* different concentrations of fluoride ions.

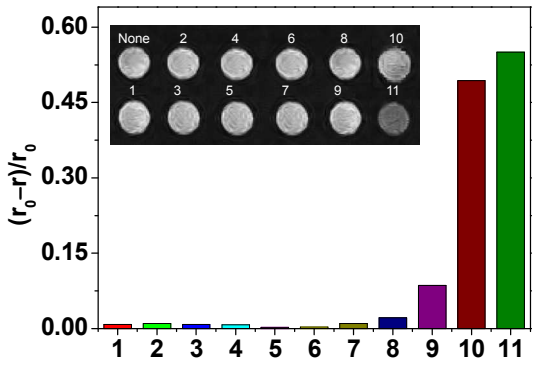

Fig. 8 Longitudinal relaxivity (r_1) responses of Gd(TTA)$_3$-**DPPZ** (0.2 mM) to various anions of interest in H_2O (THF: H_2O = 5:5, pH = 7.4). Insert: T_1-weighted MR images (T_1 measurements at a proton frequency of 20 MHz) of Gd(TTA)$_3$-**DPPZ** (0.2 m) in the presence of (1) Br^-(0.7 mM), (2) Cl^- (100 mM), (3) NO_3^-(0.7 mM), (4) OH^-(0.7 mM), (5) I^-(0.7 mM), (6) HSO_4^-(0.7 mM), (7) AcO^-(0.7 mM), (8) PO_4^{3-} (1 mM), (9) $H_2PO_4^-$(0.7 mM), (10) F^-(0.7 mM), (11) Anions mixed, respectively.

Next, we demonstrated the displacement approach by the studies on MRI response of Gd(TTA)$_3$-**DPPZ** towards fluoride ion. The MRI responses ability of Gd(TTA)$_3$-**DPPZ** (0.2 mM) toward fluoride ions were then determined using T_1 measurements at a proton frequency of 20 MHz (298 K, pH = 7.4). As shown in Fig. 7, Gd(TTA)$_3$-**DPPZ**(0.2 mM) exhibits relative stable longitudinal relaxivity (r_1 = 2.36 $mM^{-1}{\cdot}s^{-1}$) in H_2O (THF: H_2O = 5:5, pH = 7.4) arising from one inner-sphere water molecule (q = 1).[45] The relaxivity of Gd(TTA)$_3$-**DPPZ** was gradually decreased to 0.581 $mM^{-1}{\cdot}s^{-1}$ with the increase of the concentrations of fluoride ion (0–0.7 mM), which demonstrated that the replacement of coordination water with fluoride ion. Additionally, the corresponding T_1-weighted images of Gd(TTA)$_3$-**DPPZ**(0.2 mM) demonstrated a continuous decrease in spot brightness as increasing of fluoride ion concentrations (Fig. 7 insert). This together with the high longitudinal relaxivity (r_1) manifests the applicability of Gd(TTA)$_3$-**DPPZ** as an efficient T_1 MRI probe.

Interestingly, the relaxivity changes of Gd(TTA)$_3$-**DPPZ** were fluoride ion specifically over other physiologically important anions. As shown in Fig. 8, upon addition of the competitive anions (0.3 mM) including AcO^-, Br^-, Cl^-, NO_3^-, I^-, HSO_4^-, and OH^- to the solution containing Gd(TTA)$_3$-**DPPZ** (0.2 mM) does not interfere with the responses of the longitudinal relaxivity (r_1). The addition of $H_2PO_4^-$ into Gd(TTA)$_3$-**DPPZ** solution only led to slight decreasing of the longitudinal relaxivity. We reasoned that the selective MRI response of Gd(TTA)$_3$-**DPPZ** towards fluoride ion is due to the strong coordination ability of fluoride ions towards Gd(III) ions. In addition, a distinctly decreased imaging intensity in the presence of 0.3 mM fluoride ions is indeed exhibited, whereas discernible differences are not observed upon addition of equimolar amounts of AcO^-, Br^-, Cl^-, NO_3^-, I^-, HSO_4^-, OH^-, and $H_2PO_4^-$ (Fig. 8, insert).

View Article Online
DOI: 10.1039/C6DT02229D

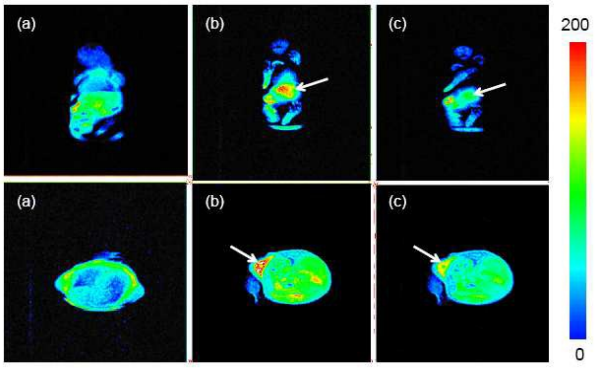

Fig. 9 *In vivo* MR pseudocolor images of living white mice. T_1-weighted MRI sagittalsection (top) and transaction (bottom) images after intraperitoneal injection of (a) None, (b) Gd(TTA)$_3$-**DPPZ** (0.2 mL, 1 mM), and (c) fluoride ions (0.2 mL, 5 mM), sequentially.

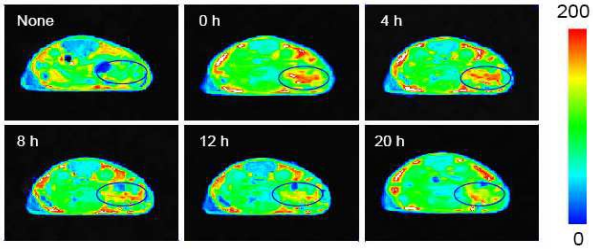

Fig. 10 *In vivo* T_1-weighted MR pseudocolor images of micepre- and post-injection of Gd(TTA)$_3$-**DPPZ** (0.4 mL, 1 mM).

Encouraged by the remarkable longitudinal relaxivity (r_1) response abilities of Gd(TTA)$_3$-**DPPZ** (0.2 mM) toward fluoride ion, we proceeded to evaluate the potential application of the contrast agent for MRI imaging *in vivo*. Prior to the MRI, the cytotoxicity of Gd(TTA)$_3$-**DPPZ** was evaluated by the reduction activity of the methyl thiazolyltetrazolium (MTT [3-(4,5-dimethylthiazol-2-yl)-2,5-diphenyltetrazolium bromide]) assay in human breast carcinoma (MDA-MB-231) cell lines. The cellular viability was estimated to be more than 50% after incubation with Gd(TTA)$_3$-**DPPZ** (1 mM) for 6 h (Fig. S8, ESI†).[46] The MRI imaging experiments were performed through intraperitoneal injection of Gd(TTA)$_3$-**DPPZ** (0.2 mL, 1 mM) into a white mice (10 g) and imaged in a 0.5 T MRI instrument. It should be noted that the injected dose of Gd(TTA)$_3$-**DPPZ** is much low than the reported MRI in mice.[47-49] As shown in Fig. 9 (b), after the injection of Gd(TTA)$_3$-**DPPZ**, a 38.5% contrast enhancement at the site of injection was observed compared with the baseline of the pre-injection image (Fig. 9 a). However, the sequentially injection of fluoride ions (0.2 mL, 5 mM) on the abdomen of the mice caused the T_1-weight MR images of the interest portions to exhibit significant contrast dark effect (Fig. 9, c). In addition, the successive bright MRI action of the Gd(TTA)$_3$-**DPPZ** on mice model was achieved at different time points, even after 20 h (Fig. 10), suggesting that the contrast agents could continuously improve contrast in tissues and have a relatively longer blood circulation time. These preliminary images demonstrate that Gd(TTA)$_3$-**DPPZ** functions successful for the MRI imaging of fluoride ion *in vivo*.

Conclusions

In this study, we presented a novel Gd(III) complex based dual modal probe, Gd(TTA)$_3$-**DPPZ** for fluoride ion sensing. Upon the addition of fluoride ions into the aqueous solution of Gd(TTA)$_3$-**DPPZ**, the replacement of the coordination water molecules led to the decreasing the longitudinal relaxivity (r_1) as well as the distinct spectroscopic changes, realizing MRI/fluorescence dual modal fluoride ion sensing. The new developed dual modal probe presents sensitively response towards fluoride ion in aqueous solution. To demonstrate its biological applications, Gd(TTA)$_3$-**DPPZ** was then successfully applied to visualise fluoride ions in abdomen of live mice by MRI images. Given these promising results, the dual modal probe reported herein may not only ensure high sensitive and selective detection of fluoride ions in aqueous solution and in biological samples, but also provide a new flexible strategy for the rational design of dual modal probes for anions sensing.

Experiment

Reagents and Instruments

All reagents and solvents were of analytical reagent grade and used without further purification unless otherwise noted. 10-phenanthroline (99%), triethylamine (99%) and o-phenylenediamine (99%) were purchased from Sinopharm Chemical Reagent Co., Ltd. (China); 2-Thenoyltrifluoroacetonate (TTA) (99%) and Gadolinium chloride ($GdCl_3$) (99.9%) were purchased from Aladdin. Tetrabutyl ammonium fluoride trihydrate (97%), tetrabutyl ammonium chloride (97%), tetrabutyl ammonium bromide (98%), tetrabutyl ammonium iodide (98%), tetrabutyl ammonium hydrogensulfate (97%), tetrabutyl ammonium dihydrogen phosphate (98%), and tetrabutyl ammonium acetate (97%) were purchased from Shanghai Chemical Reagent Co., Ltd. (China). Fresh stock solutions of anion (TBA salts, 20 mM) in H_2O were prepared for further experiments. ^{1}H-NMR and ^{13}C-NMR spectra were recorded with an AVANCE600MHZ spectrometer (BRUKER) with chemical shifts reported as *ppm* (in DMSO, TMS as internal standard). ESI-MS analyses were carried out on a HPLC-Q-Tof MS spectrometer using methanol as the eluent (Agilent). The elemental analyses of C, H, N were performed on a Vario EL III elemental analyzer. Fluorescence spectra were determined with LS 55 luminescence spectrometer (Perkin Elmer, USA). The absorption spectra were measured with a Lambda 900 UV/VIS/NIR spectrophotometer (Perkin Elmer, USA). MR imaging was performed on an MesoMR23-060H-I Analyst Analyzing & Imaging system (Shanghai Niumag Corp., China) using a 0.5 T magnet, point resolution = 256 × 128 mm, section thickness = 1 mm, TE = 18.2 ms, TR= 400 ms, and number of acquisitions = 4.

Synthesis of Gd(TTA)$_3$-DPPZ

4,5,9,14-tetraaza-benzotriphenylene (**DPPZ**) was synthesized exactly according to the literature procedure.[40] To 1,10-phenanthroline-5,6-dione (0.420 g, 2 mmol) in 20 mL of

View Article Online
DOI: 10.1039/C6DT02229D

ethanol was added o-phenylenediamine (0.238 g, 2.2 mmol) and 0.05mmolof 4-methylbenzenesulfonicacid. The mixture was heated at 80 ^{o}C for 10 h, the crude product was filtered and then recrystallized from ethanol to give the pure desired product (**DPPZ**) in 78 % yield. ^{1}H NMR (DMSO-*d*, 600 MHz) δ(*ppm*): 9.45 (d, 2H), 9.19 (d, 2H), 8.34 (d, 2H), 8.04 (d, 2H),7.91(d, 2H). ^{13}C NMR (DMSO-*d*, 150 MHz) δ(*ppm*): 152.3, 147.8, 141.6, 140.7, 133.0, 129.2, 124.5, 117.6, 114.8. ESI-MS (positive mode, m/z) Calcd for $C_{18}H_{10}N_4$: 305.0803 [**DPPZ** + Na]$^+$; Found: 305.0798.

Gd(TTA)$_3$-**DPPZ** was obtained by one-pot synthesis method according to the conventional method with minor modifications as follows.[50] TTA (0.666 g, 1 mmol) and triethylamine (3 mmol) were added to 20 mL ethanol, and stirred for 10 minutes. Then, **DPPZ** (0.282 g, 1 mmol) and gadolinium chloride (0.263 g, 1 mmol) were added. The reaction mixture was refluxed for 3 h whilst stirring to yield a yellow precipitate. After cooling to room temperature, the precipitate was washed with ethanol and dried under vacuum to obtain the targeted Gd(III) Complex, Gd(TTA)$_3$-**DPPZ** in 85% yield with a HPLC purity of 99.3%. Mp. 198.0-198.7. ESI-mass spectra (positive mode, m/z): Calcd for $C_{42}H_{22}F_9GdN_4O_6S_3$: 1102.9797; Found: 1125.9744 [Gd(TTA)$_3$-**DPPZ** + Na]$^+$, 1141.0812 [Gd(TTA)$_3$-**DPPZ** + K]$^+$, respectively. Elemental Analysis: Calculated: C, 43.86; H, 2.11; N, 5.75. Found: C, 43.63; H, 2.18; N, 5.87.

General procedures of spectra detection

Stock solutions of Gd(TTA)$_3$-**DPPZ** were prepared in mixed solution of H_2O and THF (v/v 5:5, pH = 7.4). Excitation wavelength for Gd(TTA)$_3$-**DPPZ** was 340 nm. Before spectroscopic measurements, the solution was freshly prepared by diluting the high concentration stock solution to corresponding solution (10 μM). Each time a 3 mL solution of Gd(TTA)$_3$-**DPPZ** was filled in a quartz cell of 1 cm optical path length, and different stock solutions of anions were added into the quartz cell gradually by using a micro-syringe.

Association constant calculation

Generally, for the formation of 1:1 complexation species formed by Gd(TTA)$_3$-**DPPZ** and fluoride ion, the Benesi-Hildebrand equation was used as shown below.[51]

$$\frac{1}{F - F_0} = \frac{1}{K_a(F_{max} - F_0)[F^-]} + \frac{1}{F_{max} - F_0}$$

Where F and F_0 represent the fluorescence emission at 420 nm of Gd(TTA)$_3$-**DPPZ** in the presence and absence of fluoride ion, respectively, F_{max} is the saturated fluorescence intensity of Gd(TTA)$_3$-**DPPZ** in the presence of excess amount of fluoride ions; [fluoride] is the concentration of fluoride ions added, and K_a is the binding constant.

Longitudinal relaxivity (r_1) measurements and MR imaging *in vivo*

All MR relaxivity measurements were performed on an MesoMR23-060H-I Analyst Analyzing & Imaging system (Shanghai Niumag Corp.). T_1-weighted MR images were acquired using a multi-slice gradient echo sequence. The specific relaxivity values of r_1 were calculated through the curve fitting of $1/T_1$ (s^{-1}) vs. the fluoride concentration (mM). *In vivo* MR imaging experiments were performed using a 0.5T systems. A 0.2 mL of Gd(TTA)$_3$-**DPPZ** (1 mM, DMSO: H_2O = 5:5, pH = 7.4)) was first injected into white mouse (10 g) through intraperitoneal and MR imaging was immediately followed under the Niumag 0.5 T scanner. After the MR imaging, 0.2 mL of fluoride ion (5 mM) aqueous solution was then injected into the same mice in the same place and imaged again.

Acknowledgements

This work is supported by the National Natural Science Foundation of China (No. 21301011), the Key Laboratory Program of Educational Department of Liaoning Province (LZ2015047), the State Key Laboratory of Fine Chemicals (KF1305), and the National Natural Science Foundation of China (No. 21542017).

Notes and references

1 E. L. Que and C. J. Chang, *J. Am. Chem. Soc*., 2006, **128**, 15942–15943.
2 (a) Y. Fujikawa, Y. Urano, T. Komatsu, K. Hanaoka, H. Kojima, T. Terai, H. Inoue and T. Nagano, *J. Am. Chem. Soc*., 2008, **120**, 14533–14543; (b) L. Zhang, D. Duan, Y. Liu, C. Ge, X. Cui, J. Sun and J. Fang, *J. Am. Chem. Soc*., 2014, **136**, 226–233.
3 (a) Y. T. Lim, Y.-W. Noh, J.-N. Kwon and B. H. Chung, *Chem. Commun*., 2009, 6952–6954; (b) R. Weissleder and M. J. Pittet, *Nature*, 2008, **452**, 580–589.
4 Y. Liu, K. Ai, Q. Yuan, L. Lu, *Biomaterials*, 2011,**32**, 1185–1192.
5 K. Hanaoka, K. Kikuchi, T. Terai, T. Komatsu and T. Nagano, *Chem. Eur. J*., 2008, **14**, 987– 995.
6 (a) J. L. Major, G. Parigi, C. Luchinat and T. J. Meade, *PNAS*, 2007, **104**, 13881–13886.
7 (a) A. C. Esqueda, J. A. López, G. Andreu-de-Riquer, J. C. Alvarado-Monzón, J. Ratnakar, A. J. M. Lubag, A. D. Sherry, and L. M. D. León-Rodríguez, *J. Am. Chem. Soc*., 2009, **131**, 11387–11391.
8 (a) E. Boros, E. M. Gale and P. Caravan, *Dalton Trans*., 2015, **44**, 4804–4818; (b) D. Ye, P. Pandit, P. Kempen, J. Lin, L. Xiong, R. Sinclair, B. Rutt and J. Rao, *Bioconjugate Chem*., 2014, **25**, 1526–1536.
9 K. Guo, M. Y. Berezin, J. Zheng, W. Akers, F. Lin, B. Teng, O. Vasalatiy, A. Gandjbakhche, G. L. Griffiths and S. Achilefu, *Chem. Commun*., 2010, **46**, 3705–3707.
10 (a) L. Wang, B. Li, Zhang, P. Li and H. Jiang, *Dyes and Pigment*s, 2013, **97**, 26–31; (b) Y. Yoon, B. Lee, K. Sig Lee and G. H. Im, *Adv. Funct. Mater*., 2009, **19**, 3375–3380; (c) A. B. Bourlinos, A. Bakandritsos, A. Kouloumpis, D. Gournis, M. Krysmann, E. P. Giannelis, K. Polakova, K. Safarova, K. Hola and R. Zboril, *J. Mater. Chem*., 2012, **22**, 23327–23330; (d) F. Cao, T. Huang, Y. Wang, F. Liu, L. Chen, Jun Ling, J. Sun, *Polym. Chem*., 2015, **6**, 7949–7957.
11 (a) X. L. Zhang, X. Jing, T. Liu, G. Han, H. Li and C. Y. Duan, *Inorg. Chem*., 2012, **51**, 2325−2331; (b) J. H. Jang, S. Bhuniya, J. Kang, A. Yeom, K. S. Hong and J. S. Kim. *Org. Lett*., 2013, **15**, 4702–4705.
12 (a) D. P. Dong, X. Jing, X. L. Zhang, X. Y. Hu, Y. Wu and C. Y. Duan, *Tetrahedron*, 2012, **68**, 306−310; (b) J. Luo, X.-F. Zhu and Z.-N. Chen, *Eur. J. Inorg. Chem*., 2015, 3087–3093.
13 (a) J. L. Kong, T., Y. Bao, K. Jin, X. L. Zhang, Q. Tang and C. Y. Duan, *Talanta*, 2013, **117**, 412–418; (b) W.-S. Li, J. Luo, F. Jiang and Z.-N. Chen, *Dalton Trans*., 2012, **41**, 9405–9410.

View Article Online
DOI: 10.1039/C6DT02229D

14 C. He, X. Wu, J. C. Kong, T. liu, X.L. Zhang and C. Y. Duan, *Chem. Commun*., 2012, **48**, 9290–9292.
15 H. T. Ngo, X. Liu and K. A. Jolliffe, *Chem. Soc. Rev*., 2012, **41**, 4928–4965.
16 J. W. Steed, *Chem. Soc. Rev*., 2009, **38**, 506–519.
17 A. S. Gupta, K. Paul and V. Luxami, *Spectrochimi. Acta Part A*, 2015, **138**, 67–72.
18 (a) S. Zhang, J. Fan, S. Zhang, J. Wang, X. Wang, J. Du and X. Peng, *Chem. Commun*., 2014, **50**, 14021–14024.
19 (a) K. L. Kirk, Biochemistry of the Halogens and Inorganic Halides; Plenum Press: New York, 1991; p 58; (b) M. Kleerekoper, *Endocrinol. Metab. Clin. North Am*., 1998, **27**, 441–452.
20 (a) S. A. New, J.-P. Banjour, P. Walsh, J. Mary O'Connor and J. Strain, *Nutritional Aspects of Bone Health*, 2003, 351–368; (b) S. Wen, Y. Wang and S. Dong, *RSC Adv*., 2015, **5**, 89594–89602.
21 (a) G. Waldbott, *Clin. Toxicol*., 1981, **18**, 531–541; (b) S. Matuso, K. Kiyomiya and M. Kurebe, *Arch*. *Toxicol*., 1998, **72**, 798–806.
22 B. Shi, Y. Zhang, T. Wei, Q. Lin, H. Yao, P. Zhang and X. You, *Sensors and Actuators B*, 2014, **190**, 555–561.
23 (a) L. Wang, B. Li, L. Zhang, P. Li and H. Jiang, *Dyes and Pigments*, 2013, **9**7, 26-31; (b) X. Liu, J. Xu, Y. Lv, W. Wu, W. Liu and Yu Tang, *Dalton Trans*., 2013, **4**2, 9840–9846; (b) S. Mizukami, T. Nagano, Y. Urano, A. Odani and K. Kikuchi, *J. Am. Chem. Soc*., 2002, **124**, 3920–3925.
24 (a) S. V. Eliseeva and J.-C. G. Bünzli, *Chem. Soc. Rev*., 2010, **3**9, 189–227; (b) S. Shinoda and H. Tsukube, *Analyst*, 2011, **136**, 431–435.
25 (a) S. Mizukami, K. Tonai, M. Kaneko and K. Kikuchi, *J. Am. Chem. Soc*., 2008, **130**, 14376–14377; (b) J. Yu, D. Parker, R. Pal, R. A. Poole and M. J. Cann, *J. Am. Chem. Soc*., 2006, **128**, 2294–2299.
26 (a) Y. Chen, W. Guo, Z. Ye, G. Wang and J. Yuan. *Chem. Commun.*, 2011, **47**, 6266–6268; (b) M. K. Thorson, P. Ung, F. M. Leaver, T. S. Corbin, K. L. Tuck, B. Graham and A. M. Barrios, *Anal. Chim. Acta*, 2015, **896**, 160–165.
27 (a) W. Li, Scott E. Fraser and T. J. Meade, *J. Am. Chem. Soc*., 1999, **121**, 1413–1414; (b) L. Cao, R. Zhang, W. Zhang, Z. Du, C. Liu, Z. Ye, B. Song and J. Yuan, *Biomaterials*, 2015, **68**, 21–31.
28 (a) Q. Wang, C. Tan and W. Cai, *Analyst*, 2012, **137**, 1872–1875; (b) N. Shao, J. Jin, G. Wang, Y. Zhang, R. Yang and J. Yuan, *Chem. Commun*., 2008, 1127–1129;
29 (a) D. Kasala, T.-S. Lin, C.-Y. Chen, G.-C. Liu, C.-L. Kao, T.-L. Cheng and Y.-M. Wang, *Dalton Trans*., 2011, **40**, 5018–5025; (b) I. Mamedov, N. K. Logothetis and G. Angelovski, *Org. Biomol. Chem*., 2011, **9**, 5816–5824; (c) A. C. Esqueda, J. A. López, G. Andreu-de-Riquer, J. Alvarado-Monzón, J. Ratnakar, A. J. M. Lubag, A. D. Sherry and L. M. D. León-Rodríguez, *J. Am. Chem. Soc*., 2009, **131**, 11387–11391; (d) R. Tripier, C. Platas-Iglesias, A. Boos, J.-F. Morfin and L. Charbonnière, *Eur. J. Inorg. Chem*., 2010, 2735–2745.
30 W. Li, S. E. Fraser and T. J. Meade, J. *Am. Chem. Soc*., 1999, **121**, 1413–1414.
31 (a) I. Solomon, *Phys. Rev*., 1955, **99**, 559–565; (b) N. Bloembergen, *J. Chem. Phys*., 1957, **27**, 572–573; (c) N. Bloembergen and L. O. Morgan, *J. Chem. Phys*., 1961, **34**, 842–850.
32 (a) M. E. Bartolini, J. Pekar, D. R. Chettle, F. McNeill, A. Scott, J. Sykes, F. S. Proto and G. R. Moran, *Magn. Reson. Imaging*, 2003, **21**, 541–544; (b) W. S. Li, Z. F. Li, F. Y. Jing, Y. F. Deng, L. Wei, P. Q, Liao, X. G. Yang, X. J. Li, F. K. Pei, X. X. Wang, H. Lei, *Carbohydr Res*., 2008, **343**, 685–94.
33 A. Y. Louie, M. M. Huber, E. T. Ahrens, U. Rothbacher, R. Moats, R. E. Jacobs, S. E. Fraser and T. J. Meade, *Nat. Biotechnol*., 2000, **18**, 321–325.
34 (a) J. Lin, Q. Wang, C. Tan and H. Chen, *Synth. Met*., 2010, **160**, 1780–1786; (b) D. Zhang, M. Shi, Z. Liu, F. Li, T. Yi and C. Huang, *Eur. J. Inorg. Chem*., 2006, 2277–2284.
35 (a) L. Wang, B. Li, L. Zhang, P. Li and H. Jiang, *Dyes and Pigments*, 2013,**97**, 26–31; (b) C. Yang, J. Xu, R. Zhang, Y. Zhang, Z. Li, Y. Li, L. Liang and M. Lu, *Sensors and Actuators B*, 2013, **177**, 437–444.
36 (a) Y. Zheng, C. Tan, G. P. C. Drummen and Q. Wang, *Spectrochimi. Acta Part A*, 2012, **96**, 387–394; (b) Q. Wang, C. Tan, H. Tamiaki and H. Chen, *Photochem. Photobiol. Sci*., 2010, **9**, 791–795.
37 (a) O. Sun, T. Gao, J. Sun, G. Li, H. Li, H. Xu, C. Wang and P. Yan, *CrystEngComm*, 2014, **16**, 10460–10468; (b) M. L. P. Reddy, V. Divyaa and Rani Pavithran, *Dalton Trans*., 2013, **42**, 15249–15262; (c) P. Nockemann, E. Beurer, K. Driesen, R. Van Deun, K. V. Hecke, L. V. Meervelt and K. Binnemans, *Chem. Commun*., 2005, 4354–4356.
38 (a) S. J. Butler, *Chem. Commun*., 2015, **51**, 10879–1088; (b) J. A. Tilney, T. J.Sørensen, B. P. Burton-Pyec and S. Faulkner, *Dalton Trans*., 2011, **40**, 12063–12066.
39 S. E. Plush and T. Gunnlaugsson, *Org. Lett*., 2007, **9**, 1919–1922.
40 L. Zhang and B. Li, *J. Lumin*., 2009, **129**, 1304–1308.
41 Stephen J. Butler, *Chem. Commun*., 2015, **51**, 10879–10882.
42 L. Tang and M. Cai, Sensors and Actuators B, 2012, **173**, 862–867.
43 C. Zhao, K. Qu, Y. Song, C. Xu, J. Ren and X. Qu, *Chem. Eur. J*., 2010, **16**, 8147–8154.
44 (a) Q. T. Meng, Y. Shi, C. P. Wang, H. M. Jia, X. Gao, R. Zhang, Y. F. Wang and Z. Q. Zhang, *Org. Biomol. Chem*., 2015, **13**, 2918–2926; (b) Q. T. Meng, H. M. Jia, P. Succar, L. Zhao, R. Zhang, C. Y. Duan and Z. Q. Zhang, *Biosens. Bioelectron*., 2015, **74**, 461–468.
45 P. Verwilst, S. Park, B. Yoon and J. S. Kim. *Chem. Soc. Rev*., 2015, **44**, 1791–1806.
46 Q. Meng, Y. Shi, C. Wang, H. Jia, X. Gao, R. Zhang, Y. Wang, Z. Zhang, *Org. Biomol. Chem*., 2015, **13**, 2918–2926.
47 A. Hussain, S. Saha, R. Majumdar, R. R Dighe, A. R Chakravarty, *Indian J. Chem*., 2011, **50A**, 519–530.
48 P. A. Sukerkar, K. W. MacRenaris, T. R. Townsend, R. A. Ahmed, J. E. Burdette, T. J. Meade, *Bioconjugate Chem*., 2011, **22**, 2304–2316.
49 G. J. Stasiuk, H. Smith, M. Wylezinska-Arridge, J. L. Tremoleda, W. Trigg, S. K. Luthra, V. M. Iveson, F. N. E. Gavins, N. J. Long, *Chem. Commun*., 2013, **49**, 564–566.
50 (a) D. Nie, Z. Chen, Z. Bian, J. Zhou, Z. Liu, F. Chen, Y. Zhao and C. Huang, *New J. Chem*., 2007, **31**, 1639–1646; (b) X.-N. Li, Z.-J. Wu, Z.-J. Si, L.-Z., X.-J. Liu and H.-J. Zhang, *Phys. Chem. Chem. Phys*., 2009, **11**, 9687–9695.
51 (a) Y. Wang, Z. Q. Zhang, Q. T. Meng, C. He, R. Zhang and C. Y. Duan, *J. Lumin*., 2016, **175**, 122–128; (b) Q. T. Meng, Y. Wang, M. Yang, R. Zhang, R. J. Wang and Z. Q. Zhang, *RSC Adv*., 2015, **5**, 53189–53197.

View Article Online
DOI: 10.1039/C6DT02229D

Graphical abstract

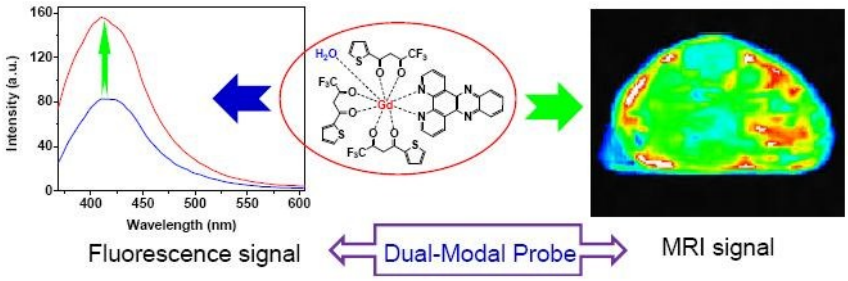

A novel Gd(III) complex based dual-modal probe, $Gd(TTA)_3$-**DPPZ** exhibits simultaneous fluorescence and longitudinal relaxivity (r_1) responses to fluoride ion (F^-) in aqueous media and *in vivo*. In the presence of fluoride ions, the replacement of the coordinated water molecules results in decreasing the longitudinal relaxivity (r_1) as well as the remarkable spectroscopic responses, thereby fluoride ion was detected by MRI/fluorescence dual bimodal modalities.